Development 135, 1681-1691 (2008) doi:10.1242/dev.017418

Critical numbers of neural crest cells are required in the pathways from the neural tube to the foregut to ensure complete enteric nervous system formation

Amanda J. Barlow*, Adam S. Wallace, Nikhil Thapar and Alan J. Burns†

The enteric nervous system (ENS) is mainly derived from vagal neural crest cells (NCC) that arise at the level of somites 1-7. To understand how the size and composition of the NCC progenitor pool affects ENS development, we reduced the number of NCC by ablating the neural tube adjacent to somites 3-6 to produce aganglionic gut. We then back-transplanted various somite lengths of quail neural tube into the ablated region to determine the 'tipping point', whereby sufficient progenitors were available for complete ENS formation. The addition of one somite length of either vagal, sacral or trunk neural tube into embryos that had the neural tube ablated adjacent to somites 3-6, resulted in ENS formation along the entire gut. Although these additional cells contributed to the progenitor pool, the quail NCC from different axial levels retained their intrinsic identities with respect to their ability to form the ENS; vagal NCC formed most of the ENS, sacral NCC contributed a limited number of ENS cells, and trunk NCC did not contribute to the ENS. As one somite length of vagal NCC was found to comprise almost the entire ENS, we ablated all of the vagal neural crest and back-transplanted one somite length of vagal neural tube from the level of somite 1 or somite 3 into the vagal region at the position of somite 3. NCC from somite 3 formed the ENS along the entire gut, whereas NCC from somite 1 did not. Intrinsic differences, such as an increased capacity for proliferation, as demonstrated in vitro and in vivo, appear to underlie the ability of somite 3 NCC to form the entire ENS.

KEY WORDS: Neural crest cell, Enteric nervous system, Gut, Hirschsprung's disease, Cell migration wave-front, Chick embryo

INTRODUCTION

The ENS in avian embryos is derived predominantly from vagal NCC that emigrate from the neural tube at the level of somites 1-7 (Burns et al., 2000; Burns and Le Douarin, 1998; Epstein et al., 1994; Le Douarin and Teillet, 1973; Yntema and Hammond, 1954). These cells exit the neural tube at embryonic day (E) 1.5 and migrate ventrally within the embryo reaching the foregut by E4, from where they then travel in a rostrocaudal direction to colonise the entire length of the gut by E8.5 (Burns, 2005; Burns and Le Douarin, 1998). Once the hindgut is colonised by vagal NCC, a second population, which delaminates from the sacral neural crest caudal to the 28th pair of somites, forms the Nerve of Remak (NoR) that extends along the dorsal wall of the gut and then enters the hindgut (Burns and Le Douarin, 1998). As the NCC migrate along the gut, they proliferate and subsequently differentiate into neurons and glia that become organised into enteric ganglia that comprise the myenteric and submucosal plexi located between the muscle layers of the gut wall (Furness, 2006).

Colonisation of the entire length of the gut by NCC is essential for the development of the ENS, as absence of enteric ganglia in the hindgut has been associated with Hirschsprung's disease (HSCR) in humans (Brooks et al., 2005; Swenson, 2002; Young et al., 2006) and aganglionic megacolon in rodents (for reviews, see Burns and Thapar, 2006; Gershon, 1999; Young et al., 2006). Therefore, any understanding of the processes that regulate NCC colonisation of the gut will further our knowledge of disease pathogenesis and may advance potential treatments for gut aganglionosis. To this end, reducing the initial number of NCC that migrate from the neural tube towards the gut by performing neural tube ablation experiments has previously been shown, by us and others (Burns et al., 2000; Peters-van der Sanden et al., 1993; Yntema and Hammond, 1954), to result in the absence of the ENS in the hindgut region, mimicking the HSCR phenotype in humans. Such experiments suggest that it is this distal region of the gut that is most sensitive to a decrease in number of migrating NCC.

Experimental data and mathematical models support the idea that specific cell-cell interactions and control of the NCC number at the migration wave-front are crucial for the advancement of NCC along the entire gut (Druckenbrod and Epstein, 2005; Druckenbrod and Epstein, 2007; Simpson et al., 2006; Simpson et al., 2007; Young et al., 2004). These data suggest that as long as the rate of proliferation of NCC at the migration wave-front, and hence cell-cell communication, is maintained, then the entire length of the gut can be colonised. Such understanding of ENS formation in both normal and disease situations has been achieved mostly by the analysis of NCC as they migrate along the length of the gut (Gianino et al., 2003; Sidebotham et al., 2002; Simpson et al., 2007; Stanchina et al., 2006; Young et al., 2005). However, there is also a need to investigate the numbers and progression of these cells, not only within the gut, but also in the migration pathways from the neural tube towards the developing foregut, regions that have, to date, received little attention in the literature. In order to understand how the initial size of the progenitor pool affects NCC migration and subsequent ENS development, we reduced the number of cells within the progenitor pool by ablating the neural tube to produce an aganglionic gut phenotype. Various somite lengths of neural tube were then back-transplanted into the ablated embryos in an effort to determine the 'tipping point', whereby sufficient progenitors were available to allow ENS formation along the length of the gut.

Neural Development Unit, UCL Institute of Child Health, London, UK.

*Present address: Stowers Institute for Medical Research, Kansas City, MO 64110, USA
†Author for correspondence (e-mail: A.Burns@ich.ucl.ac.uk)

Accepted 7 March 2008

MATERIALS AND METHODS

Animals and microsurgical manipulation

Fertile chicken (*Gallus gallus domesticus*) and quail (*Coturnix coturnix japonica*) eggs, obtained from commercial sources, were incubated at 37°C and embryos staged according to the developmental tables of Hamburger and Hamilton (Hamburger and Hamilton, 1951), or according to the number of pairs of somites formed. The gastrointestinal tract was staged according to Southwell (Southwell, 2006). Ablations were performed by microsurgically removing the neural tube, and associated neural crest, from chick embryos at the 9- to 11-somite stage (ss) of development, as previously described (Burns et al., 2000). Individual somite lengths of sacral (caudal to 28th pair of somites) or trunk (the last somite formed in 20-22ss embryos) neural tube isolated from quail embryos were grafted into chick embryos at the position of the third to fourth somite. Operated embryos were allowed to develop for a total of 2-10 days, with embryonic day (E)10 being the latest stage examined.

Immunohistochemistry

For whole embryo immunolabelling, embryos were fixed for 2 hours at room temperature (RT) in 4% paraformaldehyde in PBS then rinsed several times with PBS. They were then treated with PBS + 10% heat-inactivated sheep serum (HISS) + 0.1% Triton X-100 (blocking solution) for 3 hours at RT. Embryos were then incubated with HNK-1 (1:10 in blocking solution; ATCC) overnight at 4°C. The next day they were washed extensively in PBS then incubated overnight at 4°C with anti-mouse IgM Alexa Fluor 568 (1:500; Molecular Probes). The following day, the embryos were rinsed in PBS, mounted in Vectashield with DAPI (Vector Laboratories) and analysed with either a Leica confocal microscope, or a Zeiss Axiophot microscope with a Leica DC500 digital colour camera. Images were compiled using Adobe Photoshop software.

For whole-mount gut immunostaining, guts were fixed for 4 hours in 4% paraformaldehyde in PBS at 4°C. After washing in PBS, they were incubated for 1 hour at RT in PBS containing 10% HISS and 1% Triton X-100, rinsed in PBS, then immunostained overnight at 4°C with TuJ1 (rabbit; BABCO, 1:1000, diluted in 10% sheep serum in PBS). The following day, the guts were washed extensively in PBS, then incubated for 5 hours at RT with anti-rabbit Alexa Fluor 488 (1:500; Molecular Probes). They were then either mounted in Vectashield (Vector Laboratories) or double immunolabelled with the quail cell-specific antibody (QCPN, 1:5; Developmental Studies Hybridoma Bank) overnight at 4°C before detection with anti-mouse Alexa Fluor 568. The guts were then analysed with a Leica confocal microscope or a Leica MZFLIII fluorescence stereomicroscope. The number of isolated NC-derived cells was determined within 100 μm of the migration wave-front.

For immunolabelling of 10 μm gut cryosections, the slides were placed into blocking solution for 30 minutes before being immunostained for 5 hours at RT with TuJ1, HNK-1 (as described above), or anti-Phospho-Histone H3 (rabbit; Upstate, 1:500) and HNK-1. After washing three times with PBS, the slides were incubated with secondary antibodies (anti-mouse Alexa Fluor 488, 1:500, anti-mouse IgM Alexa Fluor 568, 1:500, or anti-rabbit Alexa Fluor 488, 1:500) in blocking solution for 2 hours at RT before being washed in PBS and mounted in Vectashield with DAPI (Vector Laboratories).

Determination of the mitotic index of NCC at the migration wave-front was performed by counting the number of Phospho-Histone H3 labelled cells within the HNK-1+ population in the first 350 μm from the most advanced cell.

Analysis of NCC proliferation and migration

To determine the proliferation of NCC in vitro, neural tube segments were isolated from quail embryos and plated onto glass coverslips coated with poly-L-lysine (Sigma) and fibronectin (Sigma). They were then incubated for 4 hours in culture media [DMEM (Invitrogen), 5% chicken embryo extract, 10% FCS (Sigma), and penicillin/streptomycin antibiotic mixture (Invitrogen), supplemented with 10 μM bromodeoxyuridine (BrdU, Sigma)] at 37°C in an atmosphere of 5% CO_2. The BrdU was then washed from the cultures and they were incubated for a further 14 hours in culture media. The following day the cultures were fixed and immunostained with anti-BrdU antibody (Oxford Biotech, UK; 1:300), as previously described (Delalande et al., 2008). The proportion of proliferating NCC was calculated and the mean distance of migration of NCC from the neural tube was determined. The significance of the difference for both proliferation and migration was determined using Student's *t*-test. These experiments were performed in triplicate, and a minimum of four samples was examined in each pair of neural tube lengths.

To determine the proliferation of grafted quail NCC in chick embryos in vivo, the embryos were allowed to develop for 2 days after grafting before being labelled for 1 hour with BrdU (10 μl/g weight of embryo of a 10 mg/ml stock solution). The embryos were then dissected, processed for cryosectioning and immunostained with QCPN as described above. Proliferating quail cells were identified by double immunohistochemistry with the anti-BrdU antibody. The percentage of proliferating quail cells and the standard error were then calculated.

RESULTS

Early migration pathways of neural crest cells: from the neural tube to the developing foregut

In order to analyse the precise spatiotemporal pathways of vagal NCC that migrate from the neural tube at the level of somites 1-7 towards and into the developing foregut, we immunostained whole embryos with the neural crest cell marker HNK-1 (Tucker et al., 1984). Examination of 11-somite stage (ss) control embryos revealed a large number of NCC on the dorsal surface migrating from the vagal region at the level of somites 1 and 2 (Fig. 1A,A′, bracketed). NCC numbers decreased rostrocaudally along the neuraxis, with very few cells present adjacent to somite 7 (Fig. 1A,A′).

At the 13 and 15ss, we observed an increase in NCC numbers (data not shown). By the 17ss, there was an extensive concentration of NCC at the base of somites 1-3, posterior to the branchial arches that abut another group of NCC that have migrated from the post-otic region of the neural tube (Fig. 1B,B′). At this stage, the greatest contribution of cells has originated from the level of somites 1-3, although there were also significant numbers of cells within somites 4 and 5. Only small numbers of NCC were apparent within the sixth somite and even fewer cells within the seventh somite (Fig. 1B,B′).

By the 27ss, NCC had migrated through the first two somites (Fig. 1C,C′), and large numbers of NCC were present within somites 3-5, with a significant grouping of NCC at their base (Fig. 1C′). Large numbers of cells were observed within the sixth and seventh somites and clusters were apparent at the base of each somite. By this stage of development, there was no apparent ventral migration of NCC within the embryo towards the foregut, rather these cells appeared to accumulate in a 'staging' area dorsal to the branchial arches (Fig. 1C,C′, bracketed).

By the 34ss, NCC had migrated through somites 1 and 2, and progressed caudally to merge with the cells at the base of the third somite (Fig. 1D,D′). There were large numbers of NCC located within somites 4 and 5, and positioned more anteriorly near the group of NCC at the base of the third somite (Fig. 1D′, arrow). Although NCC were migrating through somites 6 and 7 in large numbers, these cells were restricted within the boundary of the somite and no cells were observed collecting at the base of these somites (Fig. 1D,D′). At this stage of development (~E3), a stream of cells appeared to advance ventrally within the embryo towards the foregut from the base of somite 3 (Fig. 1D′, arrow), thus representing the first NCC to subsequently form the ENS.

Reduction in vagal neural crest cell number by microsurgical ablation

Ablation of the neural tube and associated NCC adjacent to somites 3-6 (termed hereafter, 3-6 ablated), performed between HH9 and HH11 (E1.5), resulted in the absence of NCC within and at the base

DEVELOPMENT

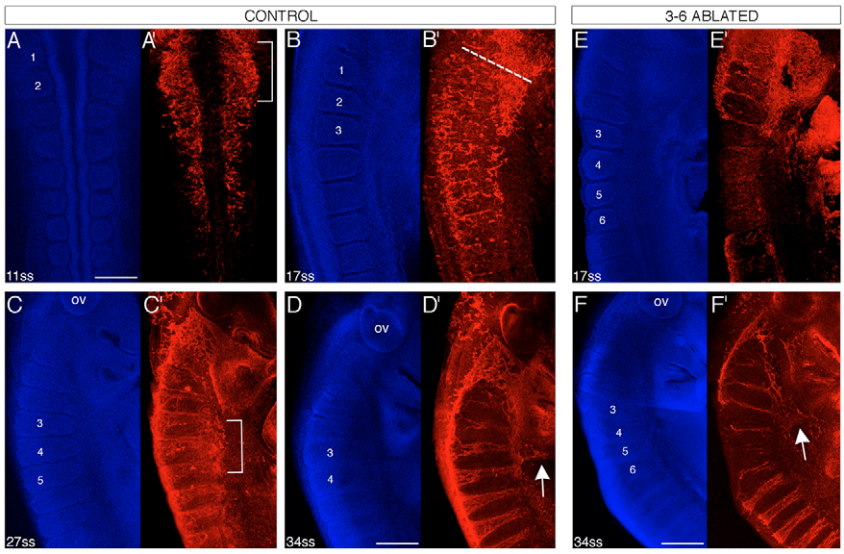

Fig. 1. HNK-1 immunohistochemistry (red) and DAPI staining (blue) of 11-34ss chick embryos. (**A**,**A′**) NCC located on the dorsal aspect of the embryo, adjacent to somites 1-2 (bracketed). (**B**,**B′**) NCC grouped at the base of somites 1-3, adjacent to an accumulation of cells arising from the post-otic region (dashed line). (**C**,**C′**) NCC concentrated at the base of somites 3-5 (bracketed). (**D**,**D′**) NCC ventral to somites 1-5. Arrow indicates cells advancing towards the foregut from the base of somite 3. (**E**,**E′**) NCC are absent from somites 3-6, and reduced in numbers in somites 1, 2 and 7. (**F**,**F′**) A small stream of NCC progressing towards the foregut (arrow). OV, otic vesicle. Scale bars: 100 μm in A, 50 μm in D and F.

of these somites by 17ss (Fig. 1E,E′). We also observed reduced numbers of NCC within somites 1 and 2, although the accumulation of NCC at the base of these somites appeared similar in number to controls (compare Fig. 1B′ and 1E′).

At the 34ss, narrow streams of NCC were present within the anterior border of somites 1-3 (Fig. 1F,F′). HNK-1+ cells were also accumulating at the base of somite 3 (Fig. 1F′, arrow), and were advancing ventrally within the embryo towards the foregut in a similar pathway to those in control embryos. Somite 6 contained NCC that appeared to have migrated from the neural tube adjacent to the most anterior limit of somite 7. These 3-6 ablated embryos contained similar numbers of NCC within somite 7 to their control counterparts (Fig. 1F,F′).

Reduction in vagal neural crest cell number by neural tube ablation adjacent to somites 3-6: progression of ENS precursors is halted in the foregut

In order to reduce the progenitor pool of NCC that subsequently enter the gut and form the ENS, the neural tube adjacent to somites 3-6 was ablated at HH stages 9 to 11 (E1.5). The guts were subsequently removed from these embryos and immunostained with the neuronal-specific antibody βIII tubulin (TuJ1) (see Fig. S1B,D,F,H in the supplementary material). As the migration wave-front of TuJ1 NC-derived cells was shown to be coincident with that identified by the NCC-specific antibody HNK-1 (see Fig. S1A,C,E,G in the supplementary material), all further studies were performed using TuJ1 to identify the developing network of ENS cells, including those at the migration wave-front.

In control embryos at E4, TuJ1+ cells had migrated through the oesophagus and stomach, and had colonised half of the length of the small intestine (SI), almost reaching the level of the umbilicus (Fig. 2A-D). Within the SI, neuronal cell bodies and axons were organised into a defined network that extended around the intestine (Fig. 2B). At the migration wave-front, TuJ1+ axons, which were highly fasciculated, projected towards the hindgut (Fig. 2D). Neuronal cell bodies were present in chain-like formations along these nerve fibres and there were few, if any, individual TuJ1+ cells not interconnected with their neighbours (Fig. 2D). By contrast, in 3-6 ablated embryos (Fig. 2E-H), TuJ1+ staining could only be detected along the initial region of the SI, with these cells colonising only 15% of its length (Fig. 3). In addition, there were fewer TuJ1+ cells in the SI, and these appeared to be spread circumferentially around the gut in a less-organised network than in controls (Fig. 2F). At the migration wave-front, neuronal cell bodies were more loosely arranged, with shorter, less fasciculated axons than those in controls, and more cells occurred in isolation (Fig. 2H, arrowheads; mean number of isolated cells in 3-6 ablated was 4.5±0.1 versus 1.0±0.3 in controls, n=6 and n=8, respectively). We also examined the number and mitotic index (MI) of NCC in consecutive cryosections of the gut, using HNK-1 and Phospho-Histone H3 at and within 350 μm of the migration wave-front [a region in which proliferation is thought to be essential for driving cells along the gut (Simpson et al., 2007)]. Although there was a 60% reduction in the absolute number of NCC in the 3-6 ablated embryos, there was no difference in the MI (double-labelled cells ÷ HNK-1-labelled cells) between control and 3-6 ablated embryos (13.5%±1.5 versus 13%±1.0, n=5).

As development progressed and the growth of the gut continued, NC-derived cells advanced along the gut, with the migration wave-front extending throughout the cecal buds and into the proximal hindgut in control guts by E7 (Fig. 2I-L, Fig. 3). A dense network of TuJ1+ staining was evident in all gut regions behind the migration wave-front (Fig. 2J,K). In 3-6 ablated embryos, the wave-front did not extend beyond the duodenum (Fig. 2N, arrow; Fig. 3). In this region, the number of cells behind the wave-front appeared to have increased (Fig. 2N) when compared with previous stages, and the extent of the intrinsic neuronal network was similar to controls.

In control embryos at E10, the entire length of the gut was occupied by NC-derived cells, with an intricate TuJ1+ network apparent in all regions of the gut (Fig. 2Q-T). However, in 3-6 ablated guts, the NC-derived cells had not progressed beyond the duodenal loop (Fig. 2V), thereby colonising only 30% of the length of the SI (Fig. 3). The NC-derived cells that had colonised the proximal part of the SI in 3-6 ablated embryos were organised into a similar cell arrangement to the control ENS (Fig. 2V). An intrinsic vagal NC-derived network was therefore absent in the midgut (Fig. 2W) and hindgut (Fig. 2X), and these regions contained only TuJ1+ cells and nerve fibres of sacral NC origin.

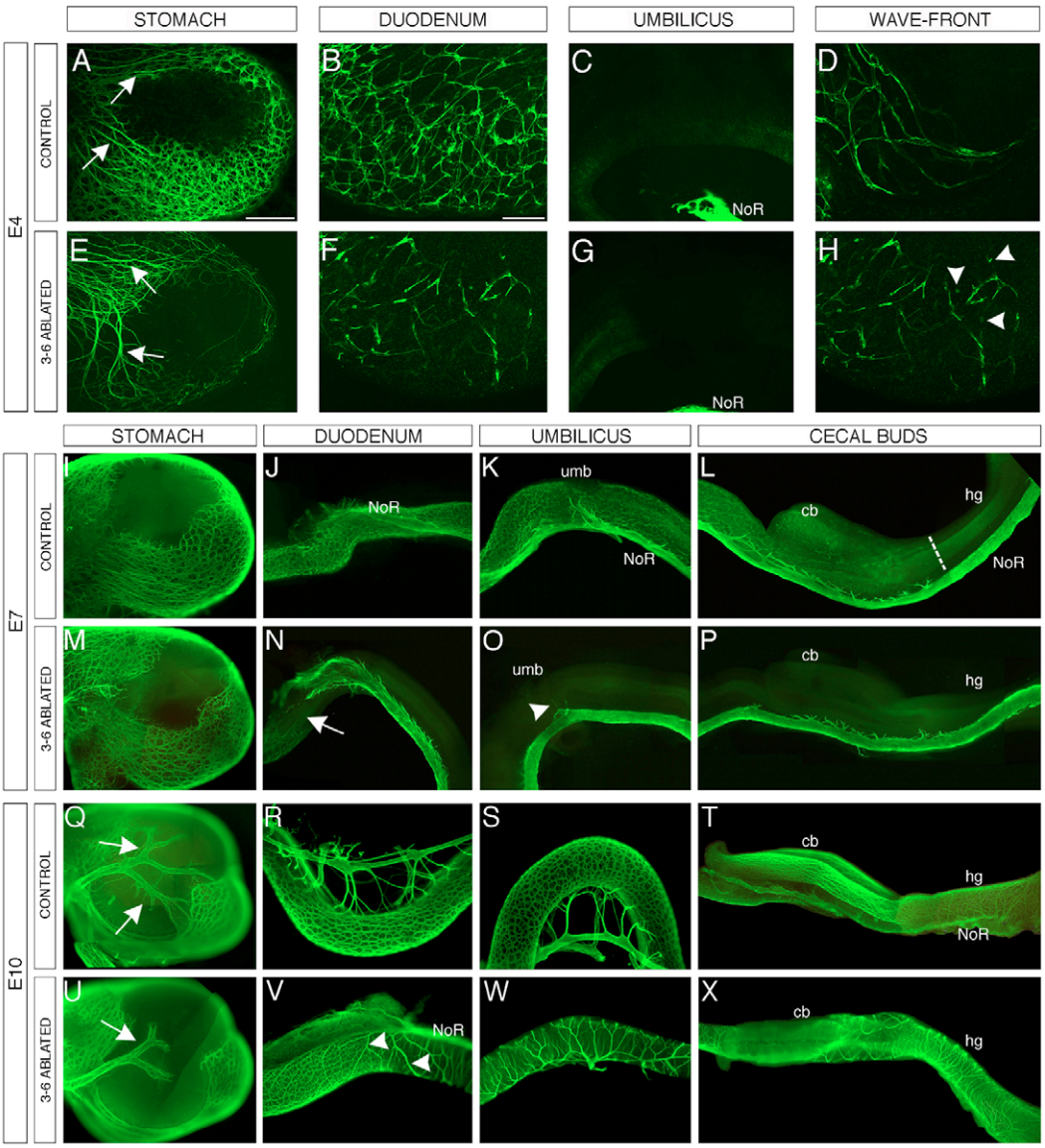

Fig. 2. TuJ1 immunostaining of E4, E7 and E10 control and 3-6 ablated whole-mount gut preparations. (**A-D**) E4 control gut showing the ENS network in (A) the stomach, where nerve fibres from the vagus nerve are apparent (arrows), and (B) the duodenum. (C) NC-derived cells are not present at the level of the umbilicus. (D) The migration wave-front contains mostly fasciculated axons and no isolated cells. (**E-H**) 3-6 ablated gut showing numerous vagus nerve fibre projections (arrows) and a reduced ENS network in (E) the stomach and (F) the duodenum. (G) NC-derived cells are not present at the level of the umbilicus and only the NoR is TuJ1+. (H) The migration wave-front has loosely organised TuJ1+ cells and more isolated cells (arrowheads). (**I-L**) Control E7 gut with characteristic TuJ1+ ENS network in (I) the stomach and (J) the duodenum. (K) At the level of the umbilicus, the NoR projects fibres into the gut wall. (L) TuJ1+ cells have migrated through the cecal buds and extend into the hindgut. NoR fibres project into the gut co-incident with the most advanced cells at the migration wave-front (dashed line). (**M-P**) 3-6 ablated gut. The TuJ1+ migration wave-front terminates at the caudal extent of the duodenum (N), which represents the anterior extent of the NoR (arrow). The umbilicus level of the intestine (O), the cecal buds and hindgut (P) do not contain NC-derived cells. (**Q-T**) E10 control gut showing characteristic ENS networks. (**U-X**) 3-6 ablated gut. There are fewer perivascular extensions (arrow) within the stomach compared with controls. (V) The caudal extent of the migration wave-front in the duodenum is co-incident with the anterior extent of the NoR. Nerve fibres project from the NoR into the gut (V, arrowheads; W,X). NoR, Nerve of Remak; umb, umbilicus; cb, cecal buds; hg, hindgut. Scale bars: 300 μm in A; 100 μm in B.

Manipulation of neural crest cell numbers: affect on progression of ENS precursors along the gut

Following the reduction in NCC numbers by ablating the neural tube adjacent to somites 3-6, the migration of NC-derived ENS precursors along the length of the gut was halted in the duodenum. In order to gain insight into the quantity of NCC required for normal colonisation of the gut, we back-transplanted varying lengths of neural tube from quail embryos into 3-6 ablated chick embryos. We initially found that two somite lengths (data not shown), and then even as little as one somite length, of neural tube (from somite 3, hereafter termed Q3) provided sufficient numbers of NCC to restore normal gut colonisation and ENS formation (Figs 4, 5).

TuJ1 staining of guts from E7, 3-6 ablated + Q3 embryos revealed an ENS network along the length of the gut that terminated at the end of the cecal buds (Fig. 4D). The extent of gut colonisation by NC-derived cells was equivalent to controls (compare Fig. 4D with

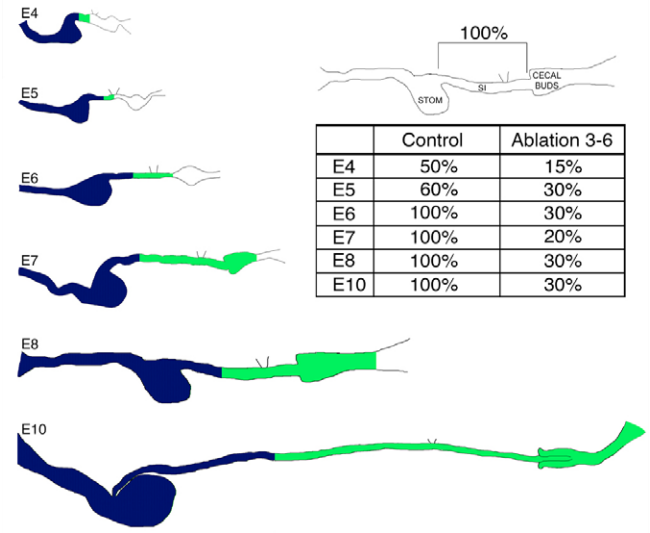

	Control	Ablation 3-6
E4	50%	15%
E5	60%	30%
E6	100%	30%
E7	100%	20%
E8	100%	30%
E10	100%	30%

Fig. 3. Schematic showing extent of gut colonisation by vagal NC-derived cells in control (green shading) and 3-6 ablated (blue shading) E4-E10 chick embryos. Table shows percentage of small intestine (SI) length colonised in control and ablated embryos. $n \geqslant 3$ at all stages examined.

Fig. 2L, n=4). The migration wave-front of quail NCC was coincident with that of the TuJ1 immunostaining (Fig. 4H), and the majority of TuJ1+ cells were of quail origin. Only a few TuJ1+ QCPN– cells were observed (see Fig. 4E-H, arrowheads).

By E10, NC-derived cells had migrated along the entire length of the 3-6 ablated + Q3 guts, similar to controls (compare Fig. 5A-D with Fig. 2Q-T, n=3). At this stage of development, the majority (i.e. more than 75%) of ENS cells appeared to be of quail origin (Fig. 5E-I).

Can neural crest cells from different axial origins contribute to the ENS progenitor pool and to subsequent ENS formation?

In order to determine whether the axial origin of the grafted NCC was crucial for the provision of NCC to the progenitor pool and subsequent colonisation of the gut, we next performed interspecies grafting of one somite length of quail neural tube from the sacral region (which normally contributes to the hindgut ENS) and trunk region (which does not normally contribute to the ENS) into the 3-6 ablated embryos.

At E10, examination of 3-6 ablated chicks that had received a one-somite-length sacral graft (3-6 ablated + Q sacral) revealed that the ENS network was present along the entire length of the gut (Fig. 5J-N, n=3). However, within the ENS network, QCPN+ NCC had only colonised the gut as far as the small intestine, caudal to the umbilicus region (Fig. 5L, n=3). These sacral (quail) cells were distributed in a rostrocaudal gradient along the gut; large numbers of QCPN+ cells were present within the duodenum (Fig. 5J), but their numbers decreased along the small intestine (Fig. 5K) and very few cells were observed in the more caudal gut regions (Fig. 5L-N).

When we grafted one somite length of quail neural tube from the trunk region into 3-6 ablated embryos (3-6 ablated + Q trunk), an ENS was also present along the entire length of the gut at E10 (Fig. 5O-S, n=5). The density of the ENS network was comparable to controls and also to the 3-6 ablated guts that had received one somite length of either vagal or sacral neural tube (compare Fig. 5O-S with Fig. 2Q-T and Fig. 5A-N, also see Table S1 in the supplementary material). However, the enteric networks in these embryos were entirely devoid of quail cells (i.e. trunk NCC), thus the ENS was comprised entirely of host NC-derived precursors (Fig. 5O-S, n=5). In these embryos, although the trunk NCC did not enter the gut, they migrated from their ectopic neural tube position towards the foregut, from where they contributed to the vagus nerves (see Fig. S2 in the supplementary material).

Can one somite length of vagal neural tube contribute sufficient NCC for ENS formation along the entire gut?

Grafting of quail somite 3 neural tube into 3-6 ablated embryos resulted in complete colonisation of the gut with the majority of the ENS network consisting of quail NCC (see Fig. 5A-I). These results suggest that either: (1) one additional somite length of vagal neural tube can provide sufficient NCC to the reduced progenitor pool that exists following 3-6 ablation to allow subsequent colonisation of the entire gut; or (2) as little as one somite length of neural tube from the vagal region has the capacity to form the entire ENS. To distinguish

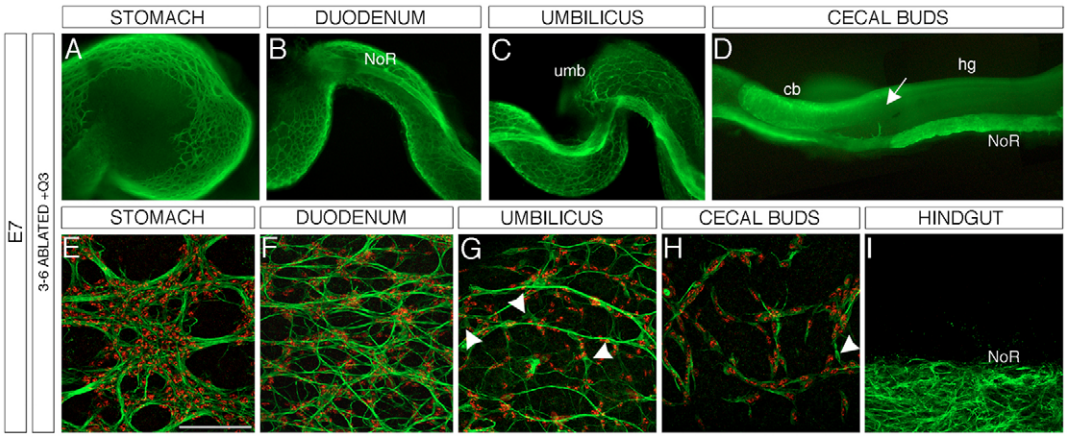

Fig. 4. TuJ1 (green) and QCPN (red) immunostaining of E7 3-6 ablated + Q3 whole-mount gut preparations. (**A-D**) TuJ1 immunolabelling of (A) stomach, (B) duodenum, (C) umbilicus and (D) the migration wave-front at the end of the cecal buds (arrow). (**E-I**) Confocal images showing the extensive contribution of quail NCC in the gut regions. The majority of TuJ1+ cells are stained with QCPN in the (E) stomach, (F) duodenum, (G) umbilicus and (H) cecal buds. Arrowheads indicate TuJ1+QCPN– cells. (I) TuJ1 immunostaining in the NoR in the hindgut. NoR, Nerve of Remak; umb, umbilicus; cb, cecal buds; hg, hindgut. Scale bar in E: 50 μm.

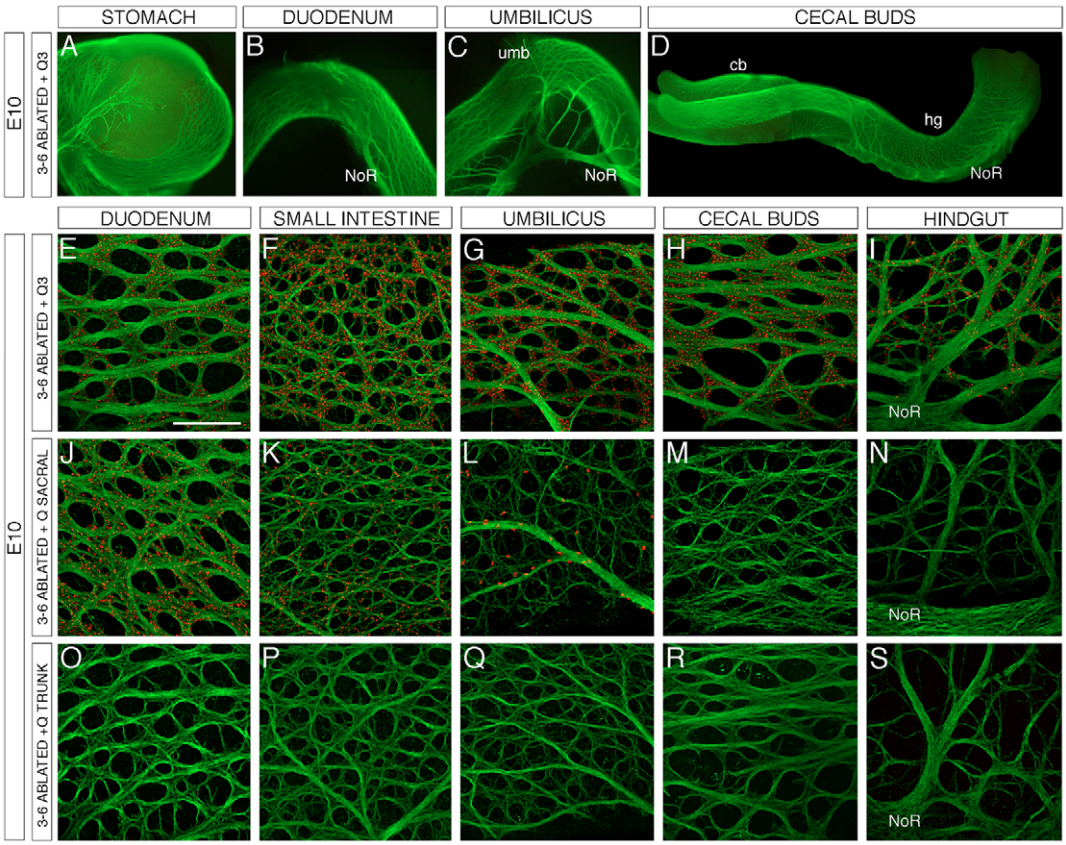

Fig. 5. TuJ1 (green) and QCPN (red) immunostaining of E10 3-6 ablated + Q3, 3-6 ablated + Q sacral and 3-6 ablated + Q trunk whole-mount gut preparations. (**A**) Characteristic ENS network and perivascular projections in the stomach. (**B**,**C**) The duodenum (B) and the umbilicus level (C) contain extensive interconnected ganglia. (**D**) The cecal buds and hindgut are completely colonised by NC-derived cells. Similar immunostaining was also observed in 3-6 ablated + Q sacral and 3-6 ablated + Q trunk guts. (**E-I**) 3-6 ablated + Q3 guts showing extensive colonisation by quail NCC within (E) the duodenum, (F) small intestine, (G) umbilicus, (H) cecal buds and (I) hindgut. (**J-N**) 3-6 ablated + Q sacral gut. The coincidence of TuJ1 and QCPN within (J) the duodenum and (K) small intestine. Fewer quail NCC were observed within the TuJ1+ ENS network. Only occasional QCPN+ cells were present within the umbilicus region (L). No quail cells were present in the cecal bud region (M) or hindgut (N). (**O-S**) Immunolabelling of 3-6 ablated + Q trunk guts reveals that there are no quail NCC throughout the entire gut. Scale bar in E: 100 μm.

between these possibilities, and to determine whether the precise vagal origin of the single somite length is critical, we ablated the entire vagal NC adjacent to somites 1-7, then back-grafted either somite 1 (which normally contributes ENS cells only to the foregut), or somite 3 (which is part of the region that forms ENS along the entire gut) vagal neural tube (Burns et al., 2000; Epstein et al., 1994), into the 1-7 ablated embryos.

Following vagal ablation, at E10 NC-derived cells were only apparent within the foregut, including the proximal duodenum, and the migration wave-front of these cells terminated in a position more rostral to that observed when 3-6 ablations were performed (Fig. 6A-D, see also Fig. S3A,B in the supplementary material; *n*=3). This phenotype has previously been observed by Yntema and Hammond (Yntema and Hammond, 1954) and Peters-van der Sanden et al. (Peters-van der Sanden et al., 1993), and the NCC present within the gut are thought to arise from neighbouring hindbrain regions. The remainder of the TuJ1 immunostaining within these guts labelled cells and nerve fibres of sacral NC origin (Fig. 6B-D, see also Fig. S3B in the supplementary material).

Upon grafting somite 1 quail neural tube into the position of the first (data not shown) or third somite of 1-7 ablated embryos (1-7 ablated + Q1), at E10 we observed a small increase in the colonisation of the gut by NC-derived cells (Fig. 6E,F). However, the migration wave-front did not extend beyond the duodenal loop in these embryos, similar to the phenotype previously described for 3-6 ablations (compare Fig. 6E-H with Fig. 2U-X, *n*=4). Behind the wave-front, the density of the ENS network was comparable to that observed in E10 control and 3-6 ablated guts (compare Fig. 6E,F and Fig. S3C in the supplementary material with Fig. 2Q,R, and 2U,V). The furthest extent of migration of the quail NCC was coincident with the TuJ1+ NC-derived migration wave-front (see Fig. S3D in the supplementary material).

Addition of somite 3 quail neural tube into the position of the first somite in 1-7 ablated embryos also produced a phenotype in which the migration wave-front did not extend beyond the duodenal loop (*n*=4, data not shown). However, when somite 3 quail neural tube was grafted into the position of the third somite in 1-7 ablated embryos (1-7 ablated + Q3) the gut was completely colonised by ENS cells, as seen by TuJ1 and QCPN immunolabelling at E10 (Fig. 6I-L, *n*=3). The density of the ENS network, and the extent of colonisation by NCC in these preparations, was similar to that observed in control and 3-6 ablated + Q3 guts (compare Fig. 6I-L and supplementary Fig. S3E,F with Fig. 2Q,R, and 2U,V).

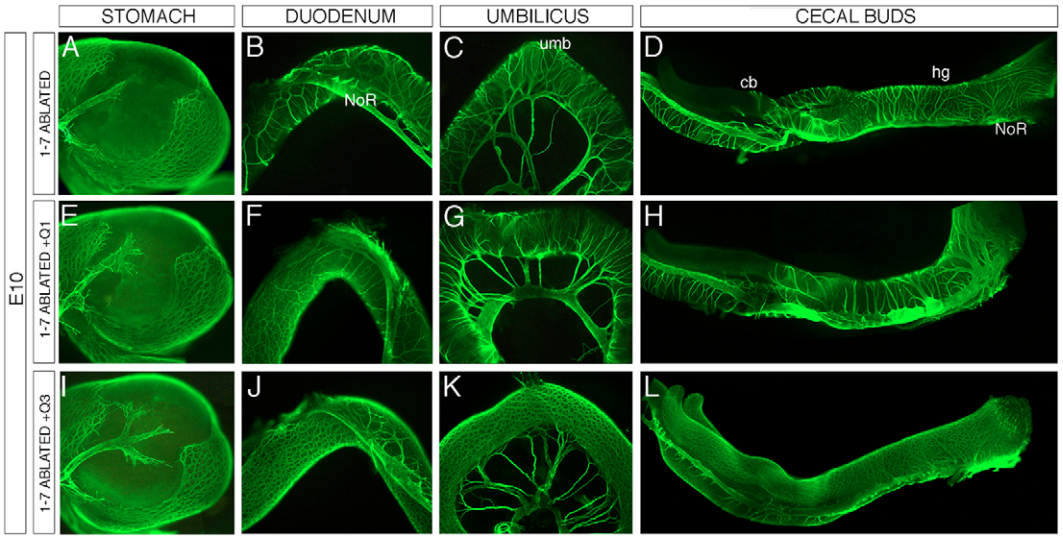

Fig. 6. TuJ1 immunohistochemistry of E10 1-7 ablated, 1-7 ablated + Q1 and 1-7 ablated + Q3 guts. (**A-D**) 1-7 ablated gut. ENS network in (A) the stomach and (B) the duodenum, which is mainly innervated by NoR fibres. The umbilicus (C) and cecal buds to the end of the terminal hindgut (D) show TuJ1 immunolabelling of the NoR and associated fibres. (**E-H**) 1-7 ablated + Q1 gut. Vagal NC-derived cells are apparent in the duodenum (F). (G,H) The umbilicus and cecal buds have immunolabelling of the NoR and associated fibres. (**I-L**) 1-7 ablated + Q3. The gut is completely colonised by vagal NC-derived cells. NoR, Nerve of Remak; umb, umbilicus; cb, cecal buds; hg, hindgut.

Migration and proliferation of vagal NCC subpopulations analysed in vitro

Ablation of the neural tube adjacent to somites 3-6 resulted in the termination of migration of NC-derived cells at the end of the duodenal loop at all stages examined, suggesting that, in these embryos, the NCC that migrate from somites 1, 2 and 7 are insufficient to colonise the entire length of the gut. In an effort to understand, mechanistically, why sub-regions of vagal NCC have different abilities to form the ENS, we analysed the migratory and proliferative capacities of different populations of vagal NCC in culture. Neural tubes adjacent to somites 1+2, 3+4 and 5+6 were dissected from quail embryos and cultured for 18 hours (Fig. 7). Calculation of the mean distance of NCC migration from the different portions of neural tubes revealed that they all have equivalent migratory potentials, such that vagal NCC adjacent to somites 1+2 migrated 410±29.2 μm (Fig. 7A,D,G), those adjacent to somites 3+4 travelled 446±24 μm (Fig. 7B,E,G), and those adjacent to somites 5+6 covered a distance of 391±15 μm (Fig. 7C,F,G; n=12 for each region examined, P>0.05). However, analysis of the incorporation of BrdU into these cultures revealed that the NCC adjacent to somites 1+2 have a reduced proliferative capacity compared with those that migrate from more caudal neural tube regions. We found that 34±1% of NCC that had migrated from the neural tube adjacent to somites 1+2 were proliferating compared with 44±2.2% and 40±3% from somites 3+4 and 5+6, respectively (compare Fig. 7D,H with Fig. 7E,F; n=12, P=0.0001 for 1+2 compared with 3+4, and P=0.02 for 1+2 compared with 5+6).

Ablation of the neural tube adjacent to somites 1-7 resulted in the termination of migration of NC-derived cells in the proximal duodenum. However, the addition of somite 3, but not somite 1, neural tube into 1-7 ablated embryos resulted in a fully formed ENS along the entire length gut. In order to understand why these individual subpopulations of NCC have differing ENS developmental potentials, we cultured these neural tube regions as described above. Results showed that somite 1 NCC proliferated less than somite 3 NCC (Fig. 7H; 30.1±2% compared with 39.5±2%, n=12, P=0.005), despite having equivalent migratory capacities (Fig. 7G; 358±17 μm versus 359±20 μm, n=12).

Analysis of proliferation in NCC transplanted in vivo

Somite 1 NCC have a reduced proliferative capacity in culture compared with somite 3 NCC. To test whether the proliferative capacity of these cells is also different in vivo, we performed 1-7 ablations of the neural tube and then grafted either somite 1 or 3 neural tube into the position of the third somite. These embryos were allowed to develop for a further two days before in vivo labelling with BrdU (Fig. 8A-F, n=3 for each neural tube addition). The NCC that had migrated from the grafted neural tube segment were identified by QCPN immunohistochemistry (Fig. 8A,C,D,F) and proliferating cells were labelled with anti-BrdU antibody (Fig. 8B,C,E,F). Analysis of the percentage of proliferating quail NCC in 1-7 ablated + Q1 and 1-7 ablated + Q3 embryos revealed that the Q1 cells proliferate significantly less than the Q3 cells (36.8±1.4% compared with 45.4±1.5%, P=0.0006). Counting of the quail NCC that had migrated from the grafted neural tube showed that, as well as the reduced proliferation of the Q1 cells, there were also 30% fewer NCC present within 1-7 ablated + Q1 embryos than within 1-7 ablated + Q3 embryos.

DISCUSSION

Here, we have shown that, when the NCC number is reduced below a critical level, the migration wave-front of ENS precursors halts at a precise boundary in the duodenum. However, the addition of as little as one somite length of vagal neural tube into 3-6 ablated embryos is sufficient to restore the NCC numbers to a critical level, or ‘tipping point’, whereby the gut is subsequently fully colonised (Fig. 9). Interestingly, in these ablated embryos, NCC from any axial origin can provide sufficient cells to the reduced precursor pool to attain the critical number required for full colonisation of the gut. Although these additional cells help to provide sufficient population pressure in

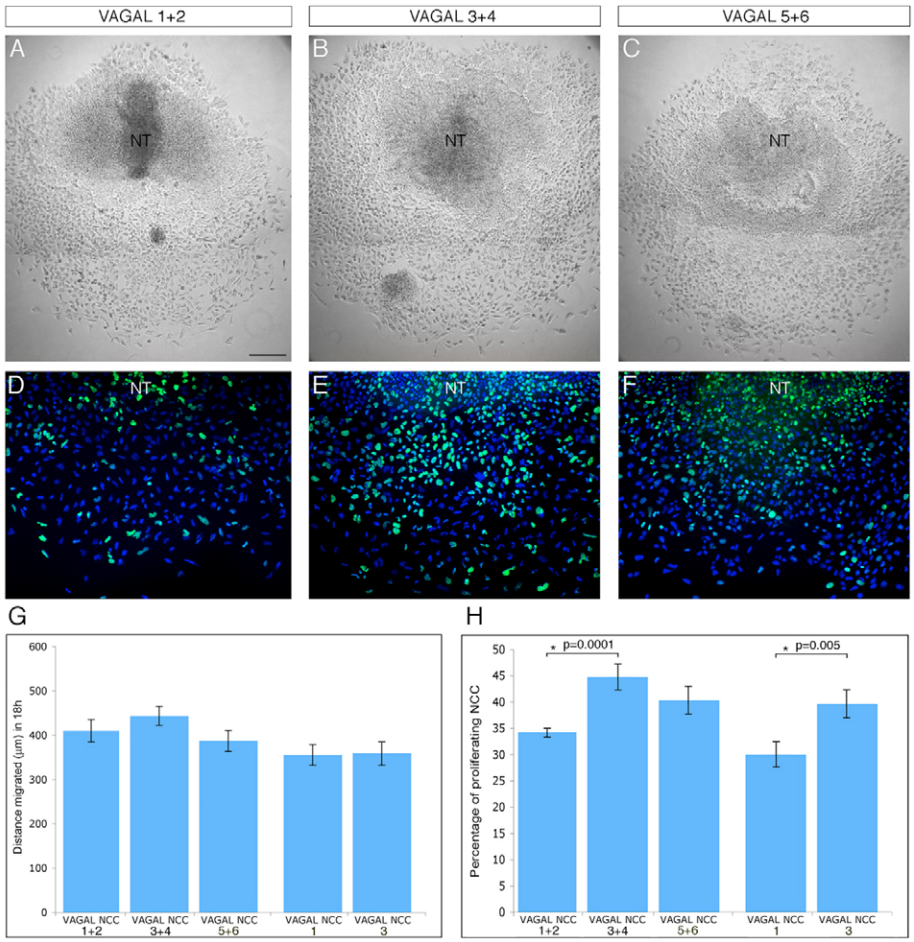

Fig. 7. Migration and proliferation of different populations of vagal NCC grown in culture for 18 hours. (**A-C**) Migration of NCC from the neural tube adjacent to (A) somites 1+2, (B) somites 3+4 and (C) somites 5+6. (**D-F**) BrdU labelling of NCC from (D) somites 1+2, (E) somites 3+4 and (F) somites 5+6. (**G**,**H**) Bar charts showing (G) the distance of migration (μm) and (H) the percentage of proliferating NCC from different somite regions. NT, neural tube. Scale bar in A: 100 μm.

the precursor pool to allow ENS formation, the NCC from different axial levels maintain their intrinsic ENS developmental potentials, such that sacral NCC contribute some cells to the ENS, whereas trunk NCC do not (see Fig. 9). We have also shown that one somite length of vagal neural tube, from the region known to colonise the entire gut, such as adjacent to somite 3 (Burns et al., 2000; Epstein et al., 1994), provides NCC that have the capacity to form the entire ENS in the absence of all other vagal crest. From in vitro proliferation and migration studies, it appears that along the vagal neuraxis, although NCC from different sub-regions migrate equivalently, there are

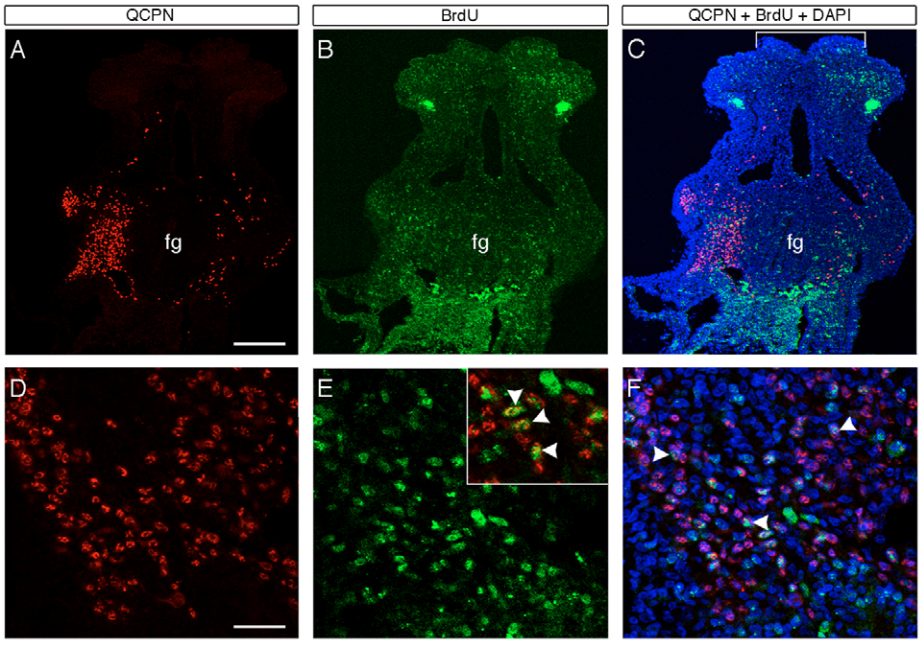

Fig. 8. QCPN (red) and BrdU (green) immunolabelling with DAPI staining (blue) of E4.5 1-7 ablated + Q3 embryos. (**A**,**D**) QCPN staining of NCC that have migrated from the grafted neural tube (not shown) towards the developing foregut. (**B**,**E**) BrdU detects proliferating cells within the embryo and within the NCC adjacent to the foregut, respectively. Inset in E shows QCPN and BrdU labelled cells. (**C**,**F**) Merged images of (C) A,B and (F) D,E with DAPI staining. Bracketed region in C shows the remnants of the neural tube following ablation. Arrowheads (E,F) indicate proliferating quail NCC. fg, foregut. Scale bars: 200 μm in A; 50 μm in D.

DEVELOPMENT

significant differences in their capacity for proliferation, with somite 3 NCC proliferating at a higher rate than those that arise adjacent to somites 1-2, a region that normally contributes ENS cells to the foregut only (Burns et al., 2000). Our findings also highlight intrinsic differences, not only in the absolute numbers of somite 3 NCC, but also in their increased capacity for proliferation in vivo, properties that could underlie the ability of this specific NCC population, and not other more rostral vagal NCC populations, to form the entire ENS.

The inability of NCC to colonise the entire gastrointestinal tract is the cause of Hirschsprung's disease (HSCR) in humans (Brooks et al., 2005; Swenson, 2002; Young et al., 2006), and mutations in a number of different genes in rodents have been shown to phenocopy this disease. More specifically, animals carrying monoisoformic alleles of the receptor tyrosine kinase gene *Ret* (*Ret*$^{51/51}$) (de Graaff et al., 2001), or mutations in the genes for endothelin receptor type B (Ednrb) and its associated ligand endothelin 3 (Edn3) (Baynash et al., 1994; Hosoda et al., 1994), or that have haploinsufficiency of the transcription factor Sox10 (Britsch et al., 2001; Herbarth et al., 1998; Southard-Smith et al., 1998), do not have NCC in the terminal region of the gut and exhibit aganglionic megacolon. Analyses of these mutant mice have focussed on the reduction in the number of NCC and their rate of migration along the gut during embryogenesis (Barlow et al., 2003; Bondurand et al., 2006; de Graaff et al., 2001; Kruger et al., 2003; Lee et al., 2003; Paratore et al., 2002; Stanchina et al., 2006; Woodward et al., 2003). Critical numbers of NCC have been shown to be required for colonisation of the entire length of the gut by other investigators who demonstrated that, when significant reductions in the number of NCC within the gut were made, the remaining NCC failed to migrate and the gut tube was left uncolonised (Peters-van der Sanden et al., 1993; Young et al., 2004). Such a critical number of NCC has been proposed to regulate specific cell-cell interactions that occur at the migration wave-front necessary for the formation of strands that are required to drive the advancement of the cells along the gut during embryonic development (Druckenbrod and Epstein, 2005; Young et al., 2004). Recent data have shown that the ability of NCC to form these strands is partly mediated by the cell adhesion molecule L1 (Anderson et al., 2006), and that it is also confined to a small region within the migratory wave-front (Druckenbrod and Epstein, 2007). NCC within 300 μm of the wave-front have also been shown to migrate faster than their more rostral neighbours (Druckenbrod and Epstein, 2007). It is clear that the NCC migration wave-front is more sensitive to the influence of the gut microenvironment, as it is these cells within *Edn3* mutants and *Gdnf* heterozygous mice that have a reduced proliferative capacity when compared with the entire population of NCC (Bondurand et al., 2006; Flynn et al., 2007). However, data against this critical number model for gut colonisation comes from the work of Sidebotham and colleagues (Sidebotham et al., 2002). These authors isolated mouse colon that contained as few as 30-100 NCC at the proximal end, and cultured the gut for 72 hours. After this time, the progeny of this small number of cells had colonised the colon to an equivalent ganglionic density to normal gut, suggesting that, at least in this region of the mouse gut, these 'leading edge' cells have a high capacity for ENS formation irrespective of their initially very low local cell density. Similar findings were obtained by Natarajan and colleagues, who injected small numbers, or even single ENS precursors, into the stomach of embryonic mouse gut that was then grown in culture (Natarajan et al., 1999). The progeny of these few cells were subsequently found throughout the gut, thus demonstrating the extensive proliferation and migration properties of enteric NCC within the gut.

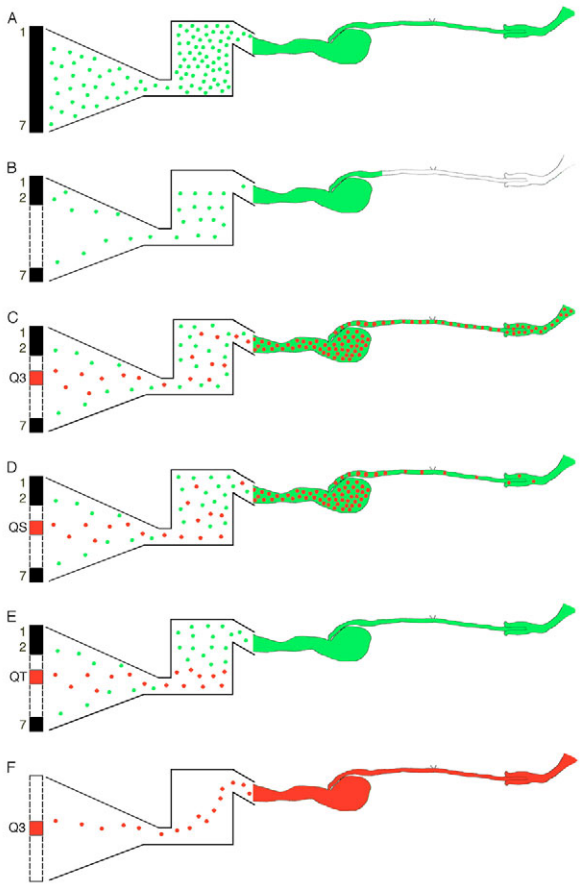

Fig. 9. Schematic showing the migration of vagal NC-derived cells (green dots and shading) and quail NCC (red dots and shading) from the neural tube towards and along the gut. (**A**) In normal embryos NCC migrate from somites 1-7, 'fill' the precursor pool, and thus have sufficient population pressure to colonise the entire length of the gut. (**B**) In 3-6 ablated embryos, the numbers of NCC in the precursor pool are reduced, such that there is insufficient population pressure to advance their migration into and along the gut. (**C**) Addition of the quail neural tube from somite 3 to 3-6 ablated embryos provides the critical number of cells to the precursor pool to allow complete colonisation of the gut. (**D**,**E**) 3-6 ablated + Q sacral (D) and 3-6 ablated + Q trunk (E) show that the sacral and trunk NCC can contribute sufficient cells to the precursor pool to enable full colonisation of the gut. The sacral NCC maintain their intrinsic identity and only contribute to the ENS in the proximal gut. Trunk NCC do not contribute any cells to the ENS, thus their role is restricted to providing critical numbers to the precursor pool to allow the remaining host vagal NCC to colonise the gut. (**F**) Grafting of somite 3 neural tube into the position of the third somite in 1-7 ablated embryos results in complete colonisation of the gut since these cells, which are more proliferative than their rostral neighbours, are placed directly into the optimal pathway to the gut.

In our experiments, when we reduced the numbers of NCC in the pathways to the gut, i.e. in 3-6 ablated embryos, we not only observed a reduction in the density of cells arranged within the neuronal networks in the duodenum, but also more individual NC-derived cells at the migration wave-front when compared with controls. These results would be expected if we reduced the NCC density to such an extent that their ability to interact with each other is altered, which would, in turn, affect the formation of the strands that are required for the advancement of NCC along the gut. An alternative explanation for

the aganglionic gut phenotype in 3-6 ablated embryos is that NCC numbers were reduced below a threshold required to produce a particular cell density that provides population pressure onto the most rostral NCC at the migration wave-front to advance their movement along the gut, a concept that was originally put forward by Newgreen and others (Newgreen et al., 1996). However, the data from our current study of 3-6 ablated embryos suggest a novel hypothesis for gut aganglionosis: a lack of critical numbers of cells along the pathways from the neural tube to the foregut may be the primary cause of the reduced migration of NCC along the length of the gut. Thus, it would appear that a critical population pressure may be required not only within the gut to move cells along its length (Newgreen et al., 1996), but, as we show here by back-transplanting small fragments of neural tube into 3-6 ablated embryos, also in the pathways from the neural tube to the foregut. Interestingly, we demonstrate that this critical number of NCC within the pathways to the gut can be provided by NCC from any axial level of the embryo, thus allowing the remaining host vagal NCC to then enter and colonise the entire length of the gut (Fig. 9). However, the NCC that migrate from the grafted tissue maintain their intrinsic identity of axial origin rather than being modified by signals within the environment. For example, quail vagal NCC were able to colonise the entire length of the gut, whereas quail sacral NCC failed to populate the hindgut when introduced to the vagal pathway, as has previously been described by Burns et al. (Burns et al., 2002). By contrast, trunk NCC were never observed within the gut upon grafting of a single somite length of trunk neural tube into 3-6 ablated embryos; these cells migrated away from the neural tube and contributed to the vagus nerves. The data for trunk NCC failing to colonise the gut are in contrast to the previous findings of Le Douarin and colleagues (Le Douarin et al., 1975; Le Douarin and Teillet, 1974), who described trunk NCC within the gut following the grafting of the trunk neural tube into the vagal region. It is possible that we did not see quail trunk NCC in guts of 3-6 ablated embryos because we did not replace the entire vagal neural tube with trunk, as carried out by the authors of this previous work (Le Douarin et al., 1975; Le Douarin and Teillet, 1974). Our recent findings also suggest that levels of Ret expression in the donor NCC from different axial levels could be critical in determining their ENS developmental potential, as sacral NCC, in which Ret was overexpressed by gene electroporation, increased their capacity for migration and became highly invasive of the hindgut (Delalande et al., 2008).

The ability of somite 3 and not somite 1 NCC to colonise the entire length of the gut further suggested that individual populations of vagal NCC have different ENS developmental potentials. We have previously shown, using quail-chick interspecies grafts, that the contribution of vagal NCC adjacent to somites 1+2 is restricted to the foregut (oesophagus and stomach), with very few cells migrating to the small intestine. By contrast, NCC from somites 3-5 colonise the entire gut from the oesophagus to terminal hindgut, whereas those from somites 6+7 colonise mainly the hindgut (Burns et al., 2000). Similar conclusions were also drawn from results obtained following retroviral labelling of somites 1-10 by Epstein et al. (Epstein et al., 1994). Vagal neural crest from somites 3-6 may therefore be uniquely 'programmed' by possessing, for example, specific signalling molecule(s) that direct these cells to colonise the entire gut. The reduced proliferative capacity of somite 1+2 NCC compared with that of 3+4 and 5+6 NCC in culture, and between somite 1 and somite 3 NCC in vivo, demonstrates that there is such an intrinsic programming of the NCC with regards to proliferation within these different vagal NCC subpopulations. However, the finding that NCC from somite 3 neural tube can form the entire ENS in 1-7 ablated embryos when grafted into the region of somite 3, but not when grafted to somite 1, also suggests that the pathways to the foregut may vary also in their 'permissiveness', with the region adjacent to somites 1-2 being sub-optimal for ENS formation compared with the adjacent vagal region.

This work was funded by a project grant from BBSRC (Biotechnology and Biological Sciences Research Council) awarded to A.J.B.

Supplementary material

Supplementary material for this article is available at
http://dev.biologists.org/cgi/content/full/135/9/1681/DC1

References

Anderson, R. B., Turner, K. N., Nikonenko, A. G., Hemperly, J., Schachner, M. and Young, H. M. (2006). The cell adhesion molecule l1 is required for chain migration of neural crest cells in the developing mouse gut. *Gastroenterology* **130**, 1221-1232.

Barlow, A., de Graaff, E. and Pachnis, V. (2003). Enteric nervous system progenitors are coordinately controlled by the G protein-coupled receptor EDNRB and the receptor tyrosine kinase RET. *Neuron* **40**, 905-916.

Baynash, A. G., Hosoda, K., Giaid, A., Richardson, J. A., Emoto, N., Hammer, R. E. and Yanagisawa, M. (1994). Interaction of endothelin-3 with endothelin-B receptor is essential for development of epidermal melanocytes and enteric neurons. *Cell* **79**, 1277-1285.

Bondurand, N., Natarajan, D., Barlow, A., Thapar, N. and Pachnis, V. (2006). Maintenance of mammalian enteric nervous system progenitors by SOX10 and endothelin 3 signalling. *Development* **133**, 2075-2086.

Britsch, S., Goerich, D. E., Riethmacher, D., Peirano, R. I., Rossner, M., Nave, K. A., Birchmeier, C. and Wegner, M. (2001). The transcription factor Sox10 is a key regulator of peripheral glial development. *Genes Dev.* **15**, 66-78.

Brooks, A. S., Oostra, B. A. and Hofstra, R. M. (2005). Studying the genetics of Hirschsprung's disease: unraveling an oligogenic disorder. *Clin. Genet.* **67**, 6-14.

Burns, A. J. (2005). Migration of neural crest-derived enteric nervous system precursor cells to and within the gastrointestinal tract. *Int. J. Dev. Biol.* **49**, 143-150.

Burns, A. J. and Le Douarin, N. M. (1998). The sacral neural crest contributes neurons and glia to the post- umbilical gut: spatiotemporal analysis of the development of the enteric nervous system. *Development* **125**, 4335-4347.

Burns, A. J. and Thapar, N. (2006). Advances in ontogeny of the enteric nervous system. *Neurogastroenterol. Motil.* **18**, 876-887.

Burns, A. J., Champeval, D. and Le Douarin, N. M. (2000). Sacral neural crest cells colonise aganglionic hindgut in vivo but fail to compensate for lack of enteric ganglia. *Dev. Biol.* **219**, 30-43.

Burns, A. J., Delalande, J. M. and Le Douarin, N. M. (2002). In ovo transplantation of enteric nervous system precursors from vagal to sacral neural crest results in extensive hindgut colonisation. *Development* **129**, 2785-2796.

de Graaff, E., Srinivas, S., Kilkenny, C., D'Agati, V., Mankoo, B. S., Costantini, F. and Pachnis, V. (2001). Differential activities of the RET tyrosine kinase receptor isoforms during mammalian embryogenesis. *Genes Dev.* **15**, 2433-2444.

Delalande, J. M., Barlow, A. J., Thomas, A. J., Wallace, A. S., Thapar, N., Erickson, C. A. and Burns, A. J. (2008). The receptor tyrosine kinase RET regulates hindgut colonization by sacral neural crest cells. *Dev. Biol.* **313**, 279-292.

Druckenbrod, N. R. and Epstein, M. L. (2005). The pattern of neural crest advance in the cecum and colon. *Dev. Biol.* **287**, 125-133.

Druckenbrod, N. R. and Epstein, M. L. (2007). Behavior of enteric neural crest-derived cells varies with respect to the migratory wavefront. *Dev. Dyn.* **236**, 84-92.

Epstein, M. L., Mikawa, T., Brown, A. M. and McFarlin, D. R. (1994). Mapping the origin of the avian enteric nervous system with a retroviral marker. *Dev. Dyn.* **201**, 236-244.

Flynn, B., Bergner, A. J., Turner, K. N., Young, H. M. and Anderson, R. B. (2007). Effect of Gdnf haploinsufficiency on rate of migration and number of enteric neural crest-derived cells. *Dev. Dyn.* **236**, 134-141.

Furness, J. B. (2006). *The Enteric Nervous System*. Oxford, UK: Blackwell Publishing.

Gershon, M. D. (1999). Lessons from genetically engineered animal models. II. Disorders of enteric neuronal development: insights from transgenic mice. *Am. J. Physiol.* **277**, G262-G267.

Gianino, S., Grider, J. R., Cresswell, J., Enomoto, H. and Heuckeroth, R. O. (2003). GDNF availability determines enteric neuron number by controlling precursor proliferation. *Development* **130**, 2187-2198.

Hamburger, V. and Hamilton, H. L. (1951). A series of normal stages in the development of chick embryo. *J. Morphol.* **88**, 49-92.

Herbarth, B., Pingault, V., Bondurand, N., Kuhlbrodt, K., Hermans-Borgmeyer, I., Puliti, A., Lemort, N., Goossens, M. and Wegner, M. (1998). Mutation of the Sry-related Sox10 gene in Dominant megacolon, a mouse

model for human Hirschsprung disease. *Proc. Natl. Acad. Sci. USA* **95**, 5161-5165.

Hosoda, K., Hammer, R. E., Richardson, J. A., Baynash, A. G., Cheung, J. C., Giaid, A. and Yanagisawa, M. (1994). Targeted and natural (piebald-lethal) mutations of endothelin-B receptor gene produce megacolon associated with spotted coat color in mice. *Cell* **79**, 1267-1276.

Kruger, G. M., Mosher, J. T., Tsai, Y. H., Yeager, K. J., Iwashita, T., Gariepy, C. E. and Morrison, S. J. (2003). Temporally distinct requirements for endothelin receptor B in the generation and migration of gut neural crest stem cells. *Neuron* **40**, 917-929.

Le Douarin, N. M. and Teillet, M. A. (1973). The migration of neural crest cells to the wall of the digestive tract in avian embryo. *J. Embryol. Exp. Morphol.* **30**, 31-48.

Le Douarin, N. M. and Teillet, M. A. (1974). Experimental analysis of the migration and differentiation of neuroblasts of the autonomic nervous system and of neurectodermal mesenchymal derivatives, using a biological cell marking technique. *Dev. Biol.* **41**, 162-184.

Le Douarin, N. M., Renaud, D., Teillet, M. A. and Le Douarin, G. H. (1975). Cholinergic differentiation of presumptive adrenergic neuroblasts in interspecific chimeras after heterotopic transplantations. *Proc. Natl. Acad. Sci. USA* **72**, 728-732.

Lee, H. O., Levorse, J. M. and Shin, M. K. (2003). The endothelin receptor-B is required for the migration of neural crest-derived melanocyte and enteric neuron precursors. *Dev. Biol.* **259**, 162-175.

Natarajan, D., Grigoriou, M., Marcos-Gutierrez, C. V., Atkins, C. and Pachnis, V. (1999). Multipotential progenitors of the mammalian enteric nervous system capable of colonising aganglionic bowel in organ culture. *Development* **126**, 157-168.

Newgreen, D. F., Southwell, B., Hartley, L. and Allan, I. J. (1996). Migration of enteric neural crest cells in relation to growth of the gut in avian embryos. *Acta Anat. (Basel)* **157**, 105-115.

Paratore, C., Eichenberger, C., Suter, U. and Sommer, L. (2002). Sox10 haploinsufficiency affects maintenance of progenitor cells in a mouse model of Hirschsprung disease. *Hum. Mol. Genet.* **11**, 3075-3085.

Peters-van der Sanden, M. J., Kirby, M. L., Gittenberger-de, Groot, A., Tibboel, D., Mulder, M. P. and Meijers, C. (1993). Ablation of various regions within the avian vagal neural crest has differential effects on ganglion formation in the fore-, mid- and hindgut. *Dev. Dyn.* **196**, 183-194.

Sidebotham, E. L., Woodward, M. N., Kenny, S. E., Lloyd, D. A., Vaillant, C. R. and Edgar, D. H. (2002). Localization and endothelin-3 dependence of stem cells of the enteric nervous system in the embryonic colon. *J. Pediatr. Surg.* **37**, 145-150.

Simpson, M. J., Landman, K. A., Hughes, B. D. and Newgreen, D. F. (2006). Looking inside an invasion wave of cells using continuum models: proliferation is the key. *J. Theor. Biol.* **243**, 343-360.

Simpson, M. J., Zhang, D. C., Mariani, M., Landman, K. A. and Newgreen, D. F. (2007). Cell proliferation drives neural crest cell invasion of the intestine. *Dev. Biol.* **302**, 553-568.

Southard-Smith, E. M., Kos, L. and Pavan, W. J. (1998). Sox10 mutation disrupts neural crest development in Dom Hirschsprung mouse model. *Nat. Genet.* **18**, 60-64.

Southwell, B. R. (2006). Staging of intestinal development in the chick embryo. *Anat. Rec. A Discov. Mol. Cell Evol. Biol.* **288**, 909-920.

Stanchina, L., Baral, V., Robert, F., Pingault, V., Lemort, N., Pachnis, V., Goossens, M. and Bondurand, N. (2006). Interactions between Sox10, Edn3 and Ednrb during enteric nervous system and melanocyte development. *Dev. Biol.* **295**, 232-249.

Swenson, O. (2002). Hirschsprung's disease: a review. *Pediatrics* **109**, 914-918.

Tucker, G. C., Aoyama, H., Lipinski, M., Tursz, T. and Thiery, J. P. (1984). Identical reactivity of monoclonal antibodies HNK-1 and NC-1: conservation in vertebrates on cells derived from the neural primordium and on some leukocytes. *Cell Differ.* **14**, 223-230.

Woodward, M. N., Sidebotham, E. L., Connell, M. G., Kenny, S. E., Vaillant, C. R., Lloyd, D. A. and Edgar, D. H. (2003). Analysis of the effects of endothelin-3 on the development of neural crest cells in the embryonic mouse gut. *J. Pediatr. Surg.* **38**, 1322-1328.

Yntema, C. L. and Hammond, W. S. (1954). The origin of intrinsic ganglia of trunk viscera from vagal neural crest in the chick embryo. *J. Comp. Neurol.* **101**, 515-541.

Young, H. M., Bergner, A. J., Anderson, R. B., Enomoto, H., Milbrandt, J., Newgreen, D. F. and Whitington, P. M. (2004). Dynamics of neural crest-derived cell migration in the embryonic mouse gut. *Dev. Biol.* **270**, 455-473.

Young, H. M., Turner, K. N. and Bergner, A. J. (2005). The location and phenotype of proliferating neural-crest-derived cells in the developing mouse gut. *Cell Tissue Res.* **320**, 1-9.

Young, H. M., Newgreen, D. and Burns, A. J. (2006). The Development of the enteric nervous system in relation to Hirschsprung's disease. In *Embryos, Genes and Birth Defects* (ed. P. Ferretti A. J. Copp C. Tickle and G. Moore), pp. 263-300. Chichester, UK: John Wiley and Sons.

Table S1. Quantitative image analysis of ENS networks following 3-6 ablation and grafting of one somite length of vagal, sacral or trunk neural tube (see Fig. 5)

	Duodenum	Small intestine	Umbilicus	Cecal buds	Hindgut
A (3-6 ablated + Q3)	62.4	59.4	47.4	56.0	55.0
B (3-6 ablated + Q Sacral)	65.5	56.3	38.7	50.9	43.4
C (3-6 ablated + Q Trunk)	54.5	62.7	51.2	56.8	37.4

To determine whether the densities of the ENS networks were significantly different between the three experimental groups (3-6 ablated + Q3, 3-6 ablated + Q sacral, 3-6 ablated + Q trunk), computerised image analysis was performed. Images were saved as Jpegs (Adobe Photoshop) and analysed using ImageJ software (www.nih.gov). The percentage area covered by TuJ1 immunohistochemical staining was measured for each region of the gut (duodenum, small intestine, umbilicus, cecal buds and hindgut) after isolating the green channel (threshold=26). Paired Student's *t*-tests were performed. Differences between the densities of ENS networks within the gut regions of each group were not statistically significant (A versus B, P=0.114; A versus C, P=0.434; B versus C, P=0.739).